

Self-gravity in neutrino-dominated accretion disks

Tong Liu^{1,2,3}, Xiao-Fei Yu¹, Wei-Min Gu¹, and Ju-Fu Lu¹

Received _____; accepted _____

arXiv:1407.0790v1 [astro-ph.HE] 3 Jul 2014

¹Department of Astronomy and Institute of Theoretical Physics and Astrophysics, Xiamen University, Xiamen, Fujian 361005, China; tongliu@xmu.edu.cn

²Key Laboratory for the Structure and Evolution of Celestial Objects, Chinese Academy of Sciences, Kunming, Yunnan 650011, China

³State Key Laboratory of Theoretical Physics, Institute of Theoretical Physics, Chinese Academy of Sciences, Beijing 100190, China

ABSTRACT

We present the effects of the self-gravity on the vertical structure and neutrino luminosity of the neutrino-dominated accretion disks in cylindrical coordinates. It is found that significant changes of the structure appear in the outer region of the disk, especially for high accretion rates (e.g., $\gtrsim 1M_{\odot} \text{ s}^{-1}$), and thus causes the slight increase of the neutrino luminosity. Furthermore, the gravitational instability of the disk is reviewed by the vertical distribution of the Toomre parameter (Toomre 1964), which may account for the late-time flares in gamma-ray bursts and the extended emission in short-duration gamma-ray bursts.

Subject headings: accretion, accretion disks - black hole physics - gamma rays burst: general - neutrinos

1. Introduction

Self-gravity has been widely investigated in accretion systems (see, e.g., Paczyński 1978a,b; Abramowicz et al. 1984; Goodman & Narayan 1988). It is easy to find that the self-gravity is important and its resulting local instabilities may develop if the mass density becomes comparable to M/R^3 , where M and R are the mass of the central object and the disk radius, respectively. The effects of the self-gravity have been considered in some interpretations of astrophysical processes. The self-gravity constraint limits the scale and angular momentum of the disk to affect the evolution of black hole mass and spin in active galactic nuclei (e.g., King et al. 2008; Hopkins & Quataert 2010). It also influences the star formation in galaxies and the formation of protostars and protostellar disks (e.g., Goodman 2003; McKee & Ostriker 2007; Rice et al. 2010).

Gamma-ray bursts (GRBs) can be sorted into two classes, i.e., short-duration and long-duration GRBs (Kouveliotou et al. 1993). Whatever types they are, the central engine of GRBs is usually considered as the system consisting of a hyperaccreting spinning stellar-mass black hole with the mass accretion rate in the range of $0.003 - 10 M_{\odot} \text{ s}^{-1}$, surrounded by a geometrically and optically thick disk with the high density and temperature, especially for the inner region ($\rho \sim 10^{10} \text{ g cm}^{-3}$, $T \sim 10^{10} \text{ K}$), namely neutrino-dominated accretion flow (NDAF). The annihilation of neutrinos escaping from the disk surface can power GRBs. This model has been studied in the past decades (see, e.g., Popham et al. 1999; Narayan et al. 2001; Di Matteo et al. 2002; Kohri & Mineshige 2002; Kohri et al. 2005; Lee et al. 2005; Gu et al. 2006; Chen & Beloborodov 2007; Kawanaka & Mineshige 2007; Kawanaka et al. 2012; Liu et al. 2007, 2008, 2010a,b, 2012a,b, 2013; Liu & Xue 2012; Pan & Yuan 2012; Xue et al. 2013). The properties of such a disk model were first worked out in details by Popham et al. (1999). The detailed microphysics and the strict hydrodynamics and thermodynamics have been considered

in some subsequent works, such as one dimensional cases (e.g., Di Matteo et al. 2002; Kohri et al. 2005; Chen & Beloborodov 2007; Janiuk et al. 2007; Kawanaka & Mineshige 2007; Liu et al. 2007; Li & Liu 2013; Xue et al. 2013) and two dimensional cases (e.g., Barkov & Baushev 2011; Janiuk et al. 2013). The dynamical features of the NDAF, such as the jet precession triggered by the system of the black hole and disk (e.g., Reynoso et al. 2006; Liu et al. 2010b; Sun et al. 2012; Hou et al. 2014a,b) can explain the quasi-periodic structure in a wide variety of observed light profiles of GRBs, and the shapes of the light curves (particularly for those with a fast rise and exponential decay or an approximate symmetry), and components features, i.e., nucleosynthesis near the surface of the disk (e.g., Fujimoto et al. 2004; Surman & McLaughlin 2004; Banerjee & Mukhopadhyay 2013; Liu et al. 2013; Xue et al. 2013), may provide a clue to understand the bumps in the optical light curve of core-collapse supernovae and the strong Fe $K\alpha$ emission lines in some GRB observations (e.g., Piro et al. 2000).

Due to the high mass density of the NDAF, we argue that the self-gravity effect may be important to the structure of the disk, and the neutrino luminosity further. Moreover, Perna et al. (2006) studied the gravitational instability in the outer parts of the hyperaccretion disk in the center of GRBs, which may result in actual fragmentation of the disk to produce energetic flares of GRBs. The vertical structure of the optically thick disk, including NDAF was investigated (e.g., Gu & Lu 2007; Liu et al. 2008; Gu et al. 2009; Jiao et al. 2009; Liu et al. 2010a), but the effects of the self-gravity and the gravitational instabilities have not been considered in these works.

In this paper, we focus on the effects of the self-gravity on the vertical structure and the neutrino luminosity of the NDAF for varying accretion rates. In Section 2, the basic equations in the vertical direction and the Toomre parameter (Toomre 1964) are introduced. The numerical results of the disk and the vertical distribution of the Toomre

parameter are presented in Section 3. Conclusions and discussion are made in Section 4.

2. Physical model

2.1. Basic equations

NDAF is one of the geometrically thick disks (e.g., Popham et al. 1999; Liu et al. 2007, 2008, 2010a) as well as the slim disk (Abramowicz et al. 1988), so its hydrodynamics and thermodynamics are expected to be similar to those of slim disks. The angular velocity Ω is approximately Keplerian, i.e., $\Omega = \Omega_K$. Thus we can write the continuity, angular momentum, and energy equations of the NDAF in cylindrical coordinates following Gu & Lu (2007) and Liu et al. (2008):

$$\dot{M} = -2\pi R\Sigma v_R = \text{constant}, \quad (1)$$

$$\dot{M}(\Omega_K R^2 - j) = 2\pi\alpha R^2 \Pi, \quad (2)$$

$$Q_{\text{vis}} = Q_{\text{adv}} + Q_{\nu}, \quad (3)$$

where \dot{M} is the mass accretion rate, v_R is the radial velocity, $\Omega_K = (GM/R)^{1/2}/(R - R_g)$ is the Keplerian angular velocity, G is the gravitation constant, $R_g = 2GM/c^2$ is the Schwarzschild radius, $j = 1.8cR_g$ is an integration constant representing the specific angular momentum accreted by the black hole, and α is the Shakura-Sunyaev viscosity parameter.

Furthermore, Σ and Π are the surface density and vertically integrated pressure, respectively, which can be defined as

$$\Sigma = 2 \int_0^\infty \rho dz, \quad (4)$$

$$\Pi = 2 \int_0^\infty p dz, \quad (5)$$

where ρ and p are the mass density and the pressure of the disk, respectively, and the sound speed is further defined as $c_s = (\Pi/\Sigma)^{1/2}$. Here we define the half thickness of the disk $H = \Sigma/2\rho_0$, where ρ_0 is the mass density on the equatorial plane.

The viscous heating rate is

$$Q_{\text{vis}} = \frac{1}{2\pi} \dot{M} \Omega_K^2 f g, \quad (6)$$

where $f = 1 - j/\Omega_K R^2$, and $g = -\text{dln}\Omega_K/\text{dln}R$. The advective cooling rate is

$$Q_{\text{adv}} = \frac{1}{2\pi} \frac{\xi \dot{M} c_s^2}{R^2}, \quad (7)$$

with $\xi = 3/2$ being a dimensionless quantity of the order of unity (e.g., Kato et al. 2008; Liu et al. 2008). The neutrino cooling is expressed by a bridging formula (e.g., Di Matteo et al. 2002; Kohri et al. 2005; Liu et al. 2007) that is valid in both the neutrino optically thin and thick regimes of the disk:

$$Q_\nu = \sum_i \frac{(7/8)\sigma T^4}{(3/4)[\tau_{\nu_i}/2 + 1/\sqrt{3} + 1/(3\tau_{a,\nu_i})]}, \quad (8)$$

where σ is the Stefan-Boltzmann constant, T is the temperature, and τ_{ν_i} is the total optical depth for neutrinos, including the absorption optical depth τ_{a,ν_i} and scattering optical depth τ_{s,ν_i} ,

$$\tau_{\nu_i} = \tau_{a,\nu_i} + \tau_{s,\nu_i}, \quad (9)$$

where the subscript i runs over the three species of neutrinos ν_e , ν_μ , and ν_τ . Here we ignore the production and distribution of the heavy elements (e.g., Di Matteo et al. 2002; Gu et al. 2006; Liu et al. 2007, 2008). The main absorption processes includes the electron-positron pair annihilation and Urca processes (e.g., Narayan et al. 2001; Di Matteo et al. 2002; Liu et al. 2007), the corresponding optical depths can be written as

$$\tau_{a,\nu_i} = 2.5 \times 10^{-7} T_{11}^5 H, \quad (10)$$

$$\tau_{a,\nu e2} = 2.5 \times 10^{-7} T_{11}^2 X_{\text{nuc}} \rho_{10} H, \quad (11)$$

where $T_{11} = T/10^{11}\text{K}$, $\rho_{10} = \rho/10^{10}\text{g cm}^{-3}$, and X_{nuc} is the mass fraction of free nucleons approximately given by (e.g., Liu et al. 2007)

$$X_{\text{nuc}} = \min\{1, 295.5 \rho_{10}^{-3/4} T_{11}^{9/8} \exp(-0.8209/T_{11})\}. \quad (12)$$

The total optical depth of scattering by nucleons can be given by

$$\tau_{s,\nu i} = 2.7 \times 10^{-7} T_{11}^2 \rho_{10} H. \quad (13)$$

The equation of state is written as (e.g., Di Matteo et al. 2002; Liu et al. 2008)

$$p = p_{\text{gas}} + p_{\text{rad}} + p_e + p_\nu. \quad (14)$$

The gas pressure from nucleons, radiation pressure of photons, degeneracy pressure of electrons, and radiation pressure of neutrinos can be expressed as $p_{\text{gas}} = (\rho k_B T / m_u)(1 + 3X_{\text{nuc}})/4$, $p_{\text{rad}} = aT^4/3$, $p_e = (2\pi hc/3)[3\rho/(16\pi m_u)]^{4/3}$, and $p_\nu = u_\nu/3$, respectively, where k_B is the Boltzmann constant, m_u is the mean mass of a nucleon, h is the Planck constant, a is the radiation density constant, and the energy density of neutrinos u_ν is (e.g., Kohri et al. 2005; Liu et al. 2007, 2008)

$$u_\nu = \sum_i \frac{(7/8)aT^4(\tau_{\nu i}/2 + 1/\sqrt{3})}{\tau_{\nu i}/2 + 1/\sqrt{3} + 1/(3\tau_{a,\nu i})}. \quad (15)$$

Moreover, we assume a polytropic relation in the vertical direction, $p = K\rho^{4/3}$, where K is a constant (Liu et al. 2008, 2010a).

If the self-gravity is considered in the NDAF model, the vertical equilibrium equation should be rewritten. We want to compare the cases considered with and without the self-gravity. The vertical equilibrium equation is given by the following three forms.

1. Case I - The form with self-gravity

As well as Paczyński (1978a,b), we define the surface density of the disk in the range from the equatorial plane to a certain height z ($z \leq H$),

$$\Sigma_z = \int_0^z \rho dz'. \quad (16)$$

If it varies slowly with radius, a new term $4\pi G\Sigma_z$ should be added in the vertical equilibrium equation, which represents the self-gravity of the disk. The equation can be written as

$$4\pi G\Sigma_z + \frac{\partial\Psi}{\partial z} + \frac{1}{\rho} \frac{\partial p}{\partial z} = 0, \quad (17)$$

where Ψ is the pseudo-Newtonian potential written by (Paczyński & Wiita 1980)

$$\Psi = -\frac{GM}{\sqrt{R^2 + z^2} - R_g}. \quad (18)$$

2. Case II - The form without self-gravity

Following Gu & Lu (2007) and Liu et al. (2008), the vertical equilibrium equation without the self-gravity can be expressed as

$$\frac{\partial\Psi}{\partial z} + \frac{1}{\rho} \frac{\partial p}{\partial z} = 0. \quad (19)$$

3. Case III - analytical form of Case I

In order to compare the cases with and without the self-gravity and indicate the vertical properties, we replace the terms of the vertical equilibrium equation in Case I [Equation (17)] with physical quantities on the equatorial plane of the disk (the subscript “0”),

$$4\pi G\rho_0 H + \Omega_K^2 H - \frac{p_0}{\rho_0 H} = 0, \quad (20)$$

which can be regarded as a reference. Moreover, the vertically integrated pressure Π is simplified as $2p_0 H$.

Finally, boundary conditions are required to numerically solve equations (2-19), which is suggested that ρ and p tend to be zero at the surface of the disk.

2.2. Toomre parameter

The matter of a differentially rotating disk is against gravitational collapse itself. The Toomre parameter can be used to measure the local gravitational stability of the accretion disks, which is expressed as

$$Q = \frac{c_s \Omega_K}{\pi G \Sigma_z}, \quad (21)$$

where $Q < 1$ implies instability. This criterion is also widely used in researches on the star formation and protostellar disks and so on. If the effects of the self-gravity are considered in the vertical structure of NDAFs, the gravitational instability should be also reviewed in the framework.

3. Numerical Results

Our results for the vertical structure and neutrino luminosity of the NDAF are shown in Figures 1-6. In all these figures, the necessary constant parameters are fixed to their most typical values, that is, $\alpha = 0.1$ and $M = 3M_\odot$.

3.1. Vertical structure

Figure 1 shows the variations of the mass density on the equatorial plane ρ_0 with radius R from $3R_g$ to $200R_g$ for $\dot{m} = 0.1, 1, 10$ ($\dot{M} = \dot{m}M_\odot \text{ s}^{-1}$). Case I, II, and III are described by the solid, dashed, and dotted lines, respectively. Figure 2 shows the variations of ρ_0 with accretion rate \dot{M} from $0.1M_\odot \text{ s}^{-1}$ to $10M_\odot \text{ s}^{-1}$ for fixed radii $10R_g$ and $100R_g$. Obviously, the effects of the self-gravity mainly reflect in the outer region of the disk, especially for the high accretion rates.

Figures 3 and 4 show that the relative thickness of the disk H/R as functions of the

radius R and accretion rate \dot{M} , respectively. We also find that the effects of the self-gravity mainly reflect in the outer region, especially for higher accretion rate. As shown in Figure 3(c), H/R in Case I is less than that in Case II by nearly an order of magnitude at $200R_g$ for $10M_\odot \text{ s}^{-1}$. We also notice that the density and the thickness have the abnormal changes in the outer region of the disk for low accretion rates. For example, when the accretion rate is $0.1M_\odot \text{ s}^{-1}$, the abnormal behaviors exist in the region outside of $50R_g$. The reason is that the degeneracy pressure of electrons, replacing the gas pressure from nucleons, dominates in the outer region for low accretion rates, i.e. $0.1M_\odot \text{ s}^{-1}$, thus causes the thickness H larger and the density ρ_0 lower in Case I than those in Case II.

Contours of the Toomre parameter with the cylindrical coordinates R and z for $\dot{m} = 0.1, 1, 10$ are shown in Figure 5. The heavy lines represent the surfaces of the disks. One end of the contours connects the disk surface and the other end tends to the equatorial plane. For the self-gravitating NDAF, it is noticed that $Q = 1$ appears at the disk surface, corresponding to $R/R_g \sim 550, 250,$ and 35 for the accretion rate $\dot{m} = 0.1, 1, 10$, and the region satisfied with $Q < 1$ is more close to the central black hole for high accretion rates.

3.2. Neutrino Luminosity

The neutrino cooling rate Q_ν can be obtained according to the above calculations, thus the neutrino radiation luminosity L_ν is expressed as

$$L_\nu = 2\pi \int_{R_{\text{in}}}^{R_{\text{out}}} Q_\nu R dR. \quad (22)$$

In our calculations, the inner and outer edge of the disk are taken to be $R_{\text{in}} = 3R_g$ and $R_{\text{out}} = 200R_g$, respectively.

Figure 6 displays the neutrino luminosity for varying \dot{m} from 0.1 to 10. We notice that the self-gravity has the limited effects on the neutrino luminosity of the NDAF. Compared

with Case II, there exists an unremarkable increase in Case I only for the high accretion rate. The physical understanding is as follows. If the neutrino trapping process can be ignored (e.g., Xue et al. 2013), the higher density and temperature exist, the more neutrinos produced. The self-gravity plays such a role to partly enhance the conditions, especially for the outer region of the NDAF. However, the inner part of the NDAF is the major neutrino emission region (e.g., Gu et al. 2006; Liu et al. 2007), the self-gravity has little influence on the region as shown in the above figures, thus there was little variation of the luminosity, even for the high accretion rate. Moreover, the descriptions of microphysics are quite important for the NDAFs, especially for the structure and components in the outer region of the disk. In our previous work, we noticed that the descriptions of microphysics have little effect on the neutrino luminosity. In Xue et al. (2013) and Li & Liu (2013), we discussed the strict microphysics as far as possible and calculate the neutrino luminosity which is close to the results under the simple equation of state (e.g., Popham et al. 1999; Di Matteo et al. 2002; Gu et al. 2006). The main physical reason is as follows. Most neutrinos are launched from the inner region of the disk, and the main components in this region are the free baryons, which completely dominate the pressure. Thus the simple or complex descriptions of the microphysics have limited influence on the state of the inner region.

4. Conclusions and discussion

In this paper we have revisited the vertical structure of NDAFs in cylindrical coordinates by including the effects of the self-gravity. It is found that the significant changes of the structure appear in the outer part of the disk, especially for high accretion rates, and thus causes the neutrino luminosity slightly enhanced. Furthermore, the vertical distribution of the Toomre parameter is reviewed, which implies that the instability may

occur in the outer region of the disk.

The criterion, $Q < 1$, indicates that the disk is gravitationally unstable, which may cause two classes of possible behavior (e.g., Perna et al. 2006). Firstly, if the local cooling of the disk is rapid, the disk may fragment into two or more parts (e.g., Nelson 2000). Since fragments form and the fall back timescale is long enough, the accretion processes will restart. This mechanism may explain the origin of late-time X-ray flares in GRBs (e.g., Luo et al. 2013), especially for short-duration GRBs corresponding to the high accretion rates in NDAFs. Secondly, the disk may evolve a quasi-steady spiral structure which can transfer angular momentum outward and mass inward. This mode can drive long-duration violent bursts if the disk mass is large enough (e.g., Lodato & Rice 2005), which may be related to the origin of GRBs with extended emissions (e.g., Liu et al. 2012b; Cao et al. 2014) or flares in long-duration GRBs.

X-ray flares are widely detected by *Swift* and other telescopes (e.g., Chincarini et al. 2007; Falcone et al. 2007). The major concern is the relation between prompt emission and flares. For example, the lag-luminosity relation for X-ray flares has been investigated (Margutti et al. 2010), and it is similar to that of the prompt emission, as well as other statistical relations, which suggests that flares may share uniform origins with prompt emission. The flare models should be followed this origination principle. In turn, the principle is the only constraint on the theoretical models.

Except for the gravitational instability, several other mechanisms have been proposed to explain the episodic X-ray flares in GRBs, such as fragmentation of a rapidly rotating core (King et al. 2005), a magnetic switch of the accretion process (Proga & Zhang 2006), differential rotation in a post-merger millisecond pulsar (Dai et al. 2006), transition of the accretion modes (Lazzati et al. 2008), outflow caused by the extreme mass accretion rates of NDAFs (Liu et al. 2008), He-synthesis-driven wind (Lee et al. 2009), jet precession

(Liu et al. 2010b; Hou et al. 2014b), dynamical instability in the jet (Lazzati et al. 2011), episodic jet produced by the magnetohydrodynamic mechanism from the accretion disk (Yuan & Zhang 2012), and so on. Thus, more information, which is from the future multi-band observations and the detections on the polarization and gravitational waves on the GRBs and their flares, should be given in order to identify these models.

We thank the anonymous referee for very useful suggestions and comments. This work was supported by the National Basic Research Program of China (973 Program) under grant 2014CB845800, the National Natural Science Foundation of China under grants 11103015, 11163003, 11222328, 11233006, 11333004, and U1331101, the CAS Open Research Program of Key Laboratory for the Structure and Evolution of Celestial Objects under grant OP201305, and the Natural Science Foundation of Fujian Province of China under grant 2012J01026.

REFERENCES

- Abramowicz, M. A., Curir, A., Schwarzenberg-Czerny, A., & Wilson, R. E. 1984, MNRAS, 208, 279
- Abramowicz, M. A., Czerny, B., Lasota, J.-P., & Szuszkiewicz, E. 1988, ApJ, 332, 646
- Banerjee, I., & Mukhopadhyay, B. 2013, ApJ, 778, 8
- Barkov, M. V., & Baushev, A. N. 2011, New A, 16, 46
- Cao, X., Liang, E.-W., & Yuan, Y.-F. 2014, arXiv:1405.7097
- Chen, W.-X., & Beloborodov, A. M. 2007, ApJ, 657, 383
- Chincarini, G., Moretti, A., Romano, P., et al. 2007, ApJ, 671, 1903
- Dai, Z. G., Wang, X. Y., Wu, X. F., & Zhang, B. 2006, Science, 311, 1127
- Di Matteo, T., Perna, R., & Narayan, R. 2002, ApJ, 579, 706
- Falcone, A. D., Morris, D., Racusin, J., et al. 2007, ApJ, 671, 1921
- Fujimoto, S.-i., Hashimoto, M.-a., Arai, K., & Matsuba, R. 2004, ApJ, 614, 847
- Goodman, J. 2003, MNRAS, 339, 937
- Goodman, J., & Narayan, R. 1988, MNRAS, 231, 97
- Gu, W.-M., Liu, T., & Lu, J.-F. 2006, ApJ, 643, L87
- Gu, W.-M., & Lu, J.-F. 2007, ApJ, 660, 541
- Gu, W.-M., Xue, L., Liu, T., & Lu, J.-F. 2009, PASJ, 61, 1313
- Hopkins, P. F., & Quataert, E. 2010, MNRAS, 407, 1529

- Hou, S.-J., Gao, H., Liu, T., et al. 2014, MNRAS, 441, 2375
- Hou, S.-J., Liu, T., Gu, W.-M., et al. 2014, ApJ, 781, L19
- Janiuk, A., Mioduszewski, P., & Moscibrodzka, M. 2013, ApJ, 776, 105
- Janiuk, A., Yuan, Y., Perna, R., & Di Matteo, T. 2007, ApJ, 664, 1011
- Jiao, C.-L., Xue, L., Gu, W.-M., & Lu, J.-F. 2009, ApJ, 693, 670
- Kato, S., Fukue, J., & Mineshige, S. 2008, Black-Hole Accretion Disks: Towards a New Paradigm, Kyoto University Press (Kyoto, Japan)
- Kawanaka, N., & Mineshige, S. 2007, ApJ, 662, 1156
- Kawanaka, N., Piran, T., & Krolik, J. H. 2013, ApJ, 766, 31
- King, A., O'Brien, P. T., Goad, M. R., et al. 2005, ApJ, 630, L113
- King, A. R., Pringle, J. E., & Hofmann, J. A. 2008, MNRAS, 385, 1621
- Kohri, K., & Mineshige, S. 2002, ApJ, 577, 311
- Kohri, K., Narayan, R., & Piran, T. 2005, ApJ, 629, 341
- Kouveliotou, C., Meegan, C. A., Fishman, G. J., et al. 1993, ApJ, 413, L101
- Lazzati, D., Blackwell, C. H., Morsony, B. J., & Begelman, M. C. 2011, MNRAS, 411, L16
- Lazzati, D., Perna, R., & Begelman, M. C. 2008, MNRAS, 388, L15
- Lee, W. H., Ramirez-Ruiz, E., & López-Cámara, D. 2009, ApJ, 699, L93
- Lee, W. H., Ramirez-Ruiz, E., & Page, D. 2005, ApJ, 632, 421
- Li, A., & Liu, T. 2013, A&A, 555, A129

- Liu, T., Gu, W.-M., Dai, Z.-G., & Lu, J.-F. 2010a, *ApJ*, 709, 851
- Liu, T., Gu, W.-M., Xue, L., & Lu, J.-F. 2007, *ApJ*, 661, 1025
- Liu, T., Gu, W.-M., Xue, L., & Lu, J.-F. 2012a, *Ap&SS*, 337, 711
- Liu, T., Gu, W.-M., Xue, L., Weng, S.-S., & Lu, J.-F. 2008, *ApJ*, 676, 545
- Liu, T., Liang, E.-W., Gu, W.-M., et al. 2010b, *A&A*, 516, A16
- Liu, T., Liang, E.-W., Gu, W.-M., et al. 2012b, *ApJ*, 760, 63
- Liu, T., & Xue, L. 2012, *Science China Physics, Mechanics, and Astronomy*, 55, 316
- Liu, T., Xue, L., Gu, W.-M., & Lu, J.-F. 2013, *ApJ*, 762, 102
- Lodato, G., & Rice, W. K. M. 2005, *MNRAS*, 358, 1489
- Luo, Y., Gu, W.-M., Liu, T., & Lu, J.-F. 2013, *ApJ*, 773, 142
- Margutti, R., Guidorzi, C., Chincarini, G., et al. 2010, *MNRAS*, 406, 2149
- McKee, C. F., & Ostriker, E. C. 2007, *ARA&A*, 45, 565
- Narayan, R., Piran, T., & Kumar, P. 2001, *ApJ*, 557, 949
- Nelson, C. H. 2000, *ApJ*, 544, L91
- Paczynski, B. 1978, *Acta Astron.*, 28, 91
- Paczynski, B. 1978, *Acta Astron.*, 28, 241
- Paczynski, B., & Wiita, P. J. 1980, *A&A*, 88, 23
- Pan, Z., & Yuan, Y.-F. 2012, *ApJ*, 759, 82
- Perna, R., Armitage, P. J., & Zhang, B. 2006, *ApJ*, 636, L29

- Piro, L., Garmire, G., Garcia, M., et al. 2000, *Science*, 290, 955
- Popham, R., Woosley, S. E., & Fryer, C. 1999, *ApJ*, 518, 356
- Proga, D., & Zhang, B. 2006, *MNRAS*, 370, L61
- Reynoso, M. M., Romero, G. E., & Sampayo, O. A. 2006, *A&A*, 454, 11
- Rice, W. K. M., Mayo, J. H., & Armitage, P. J. 2010, *MNRAS*, 402, 1740
- Sun, M.-Y., Liu, T., Gu, W.-M., & Lu, J.-F. 2012, *ApJ*, 752, 31
- Surman, R., & McLaughlin, G. C. 2004, *ApJ*, 603, 611
- Toomre, A. 1964, *ApJ*, 139, 1217
- Xue, L., Liu, T., Gu, W.-M., & Lu, J.-F. 2013, *ApJS*, 207, 23
- Yuan, F., & Zhang, B. 2012, *ApJ*, 757, 56

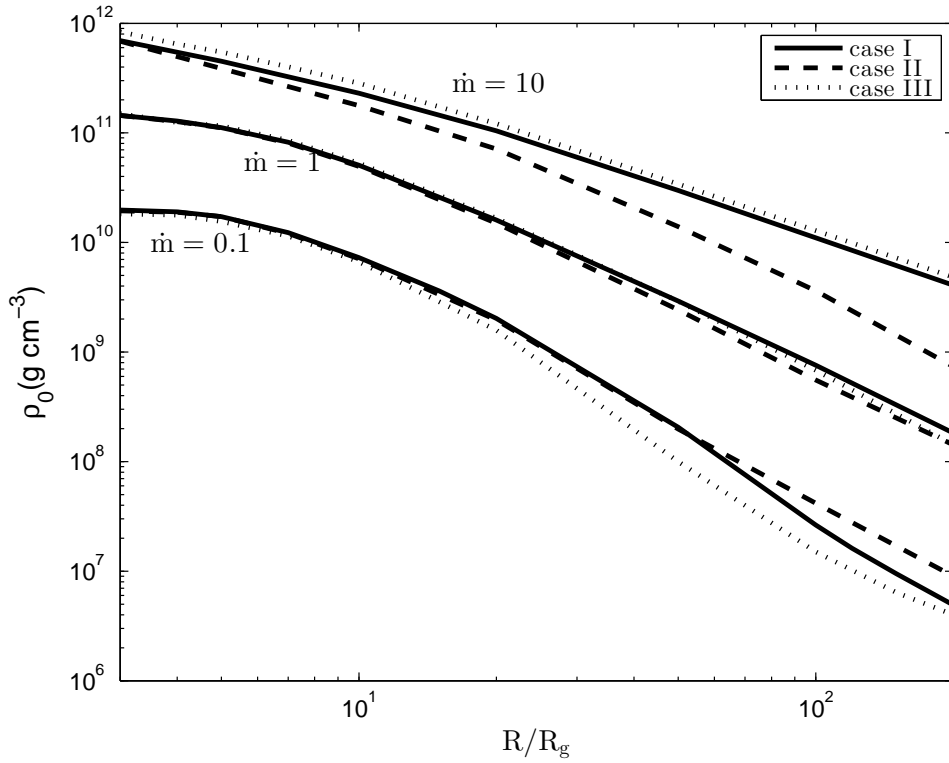


Fig. 1.— Variations of the mass density on the equatorial plane ρ_0 with radius R for $\dot{m} = 0.1, 1, 10$ ($\dot{M} = \dot{m}M_\odot \text{ s}^{-1}$). Case I, II, and III are described by the solid, dashed, and dotted lines, respectively (similarly hereafter).

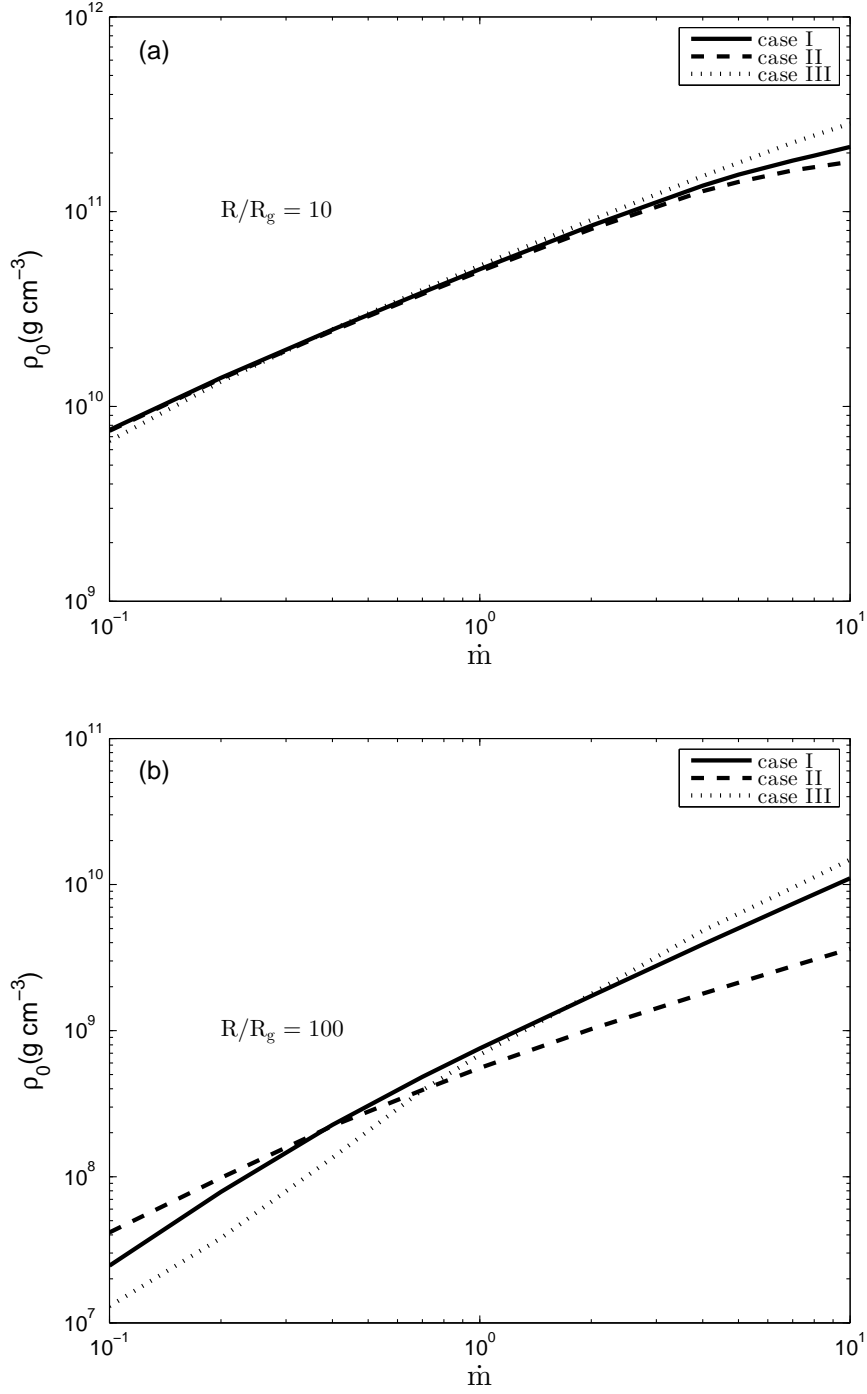


Fig. 2.— Variations of ρ_0 with accretion rate \dot{m} at $R = 10R_g$ and $100R_g$.

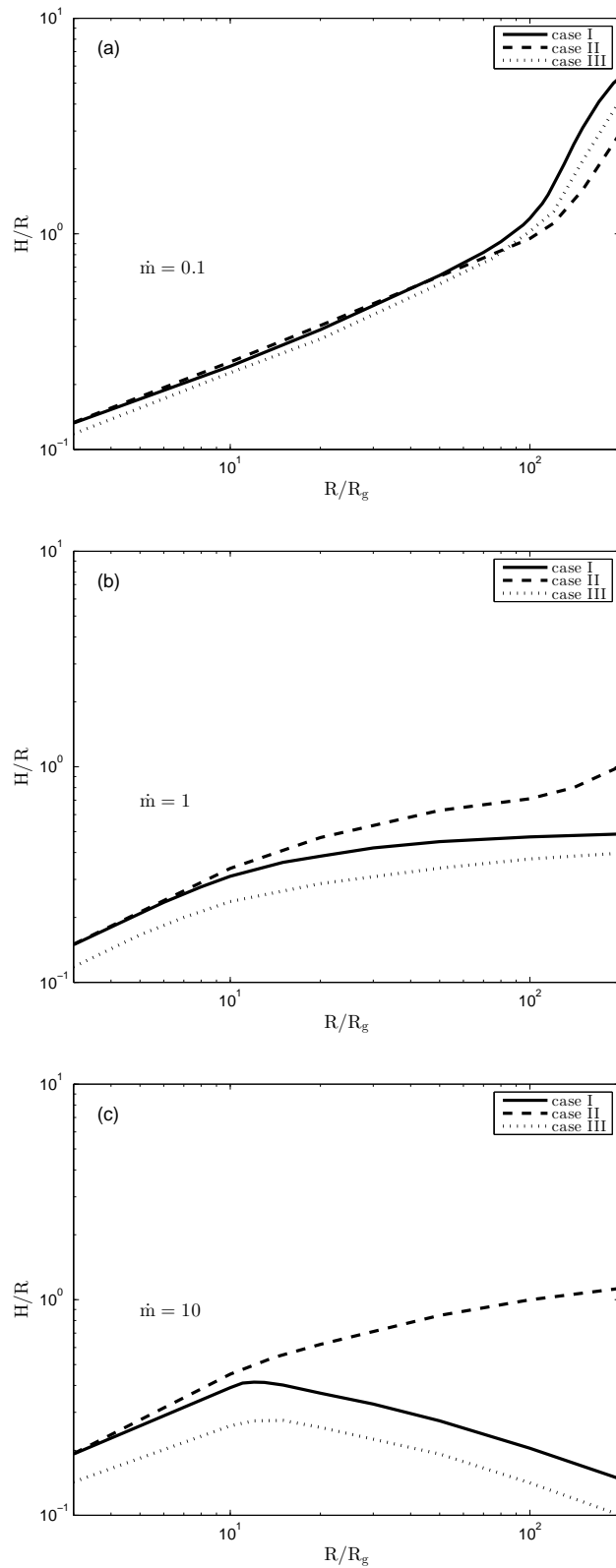


Fig. 3.— Relative thickness H/R as a function of R for $\dot{m} = 0.1, 1, 10$.

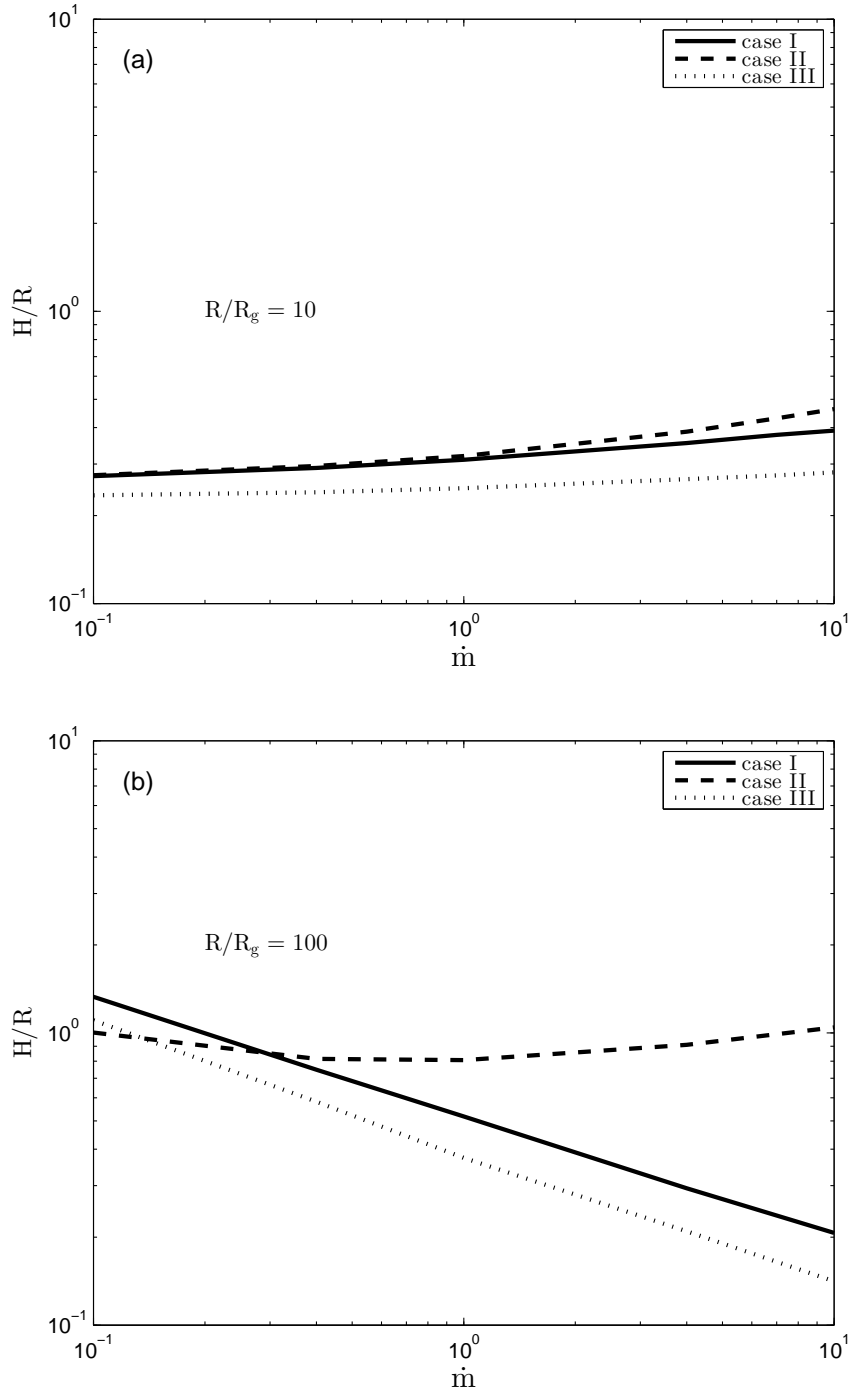


Fig. 4.— Relative thickness H/R for varying accretion rate \dot{m} from 0.1 to 10 for fixed radii $10R_g$ and $100R_g$.

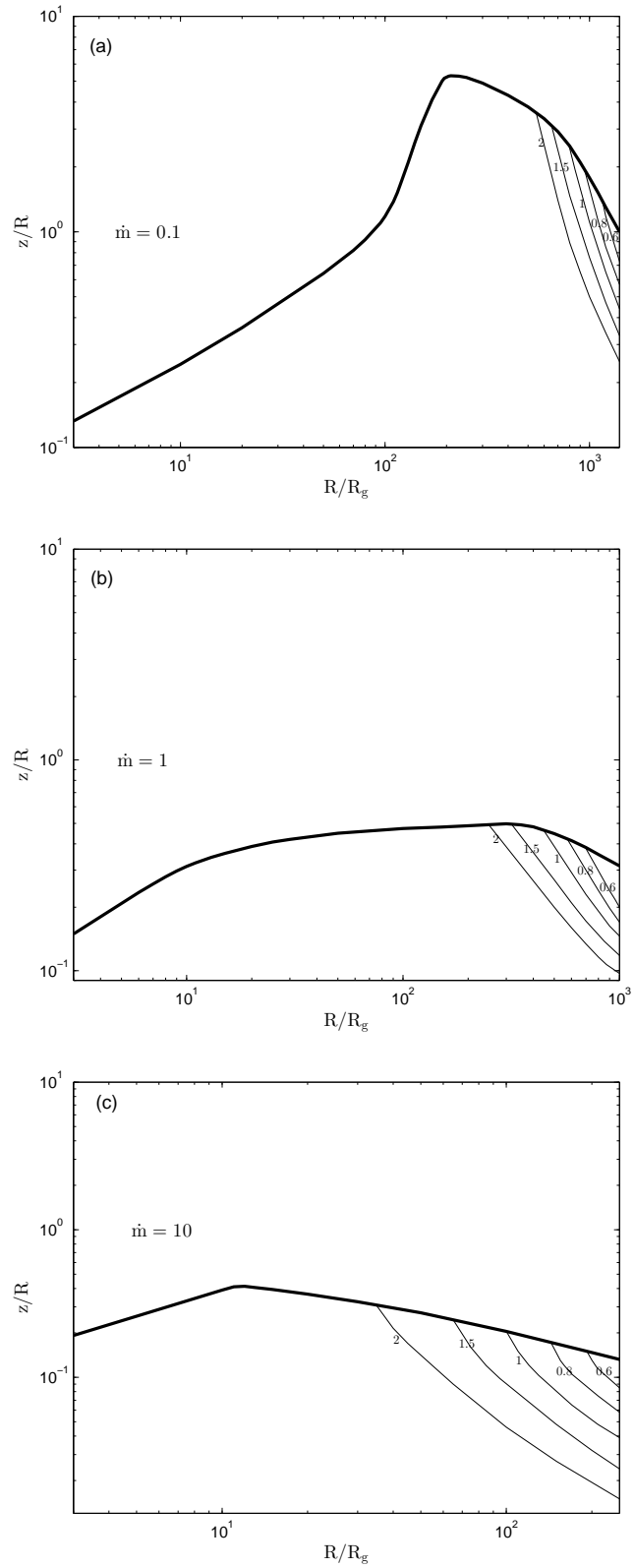


Fig. 5.— Contours of Toomre parameter with cylindrical coordinates R and z for $\dot{m} = 0.1, 1, 10$.

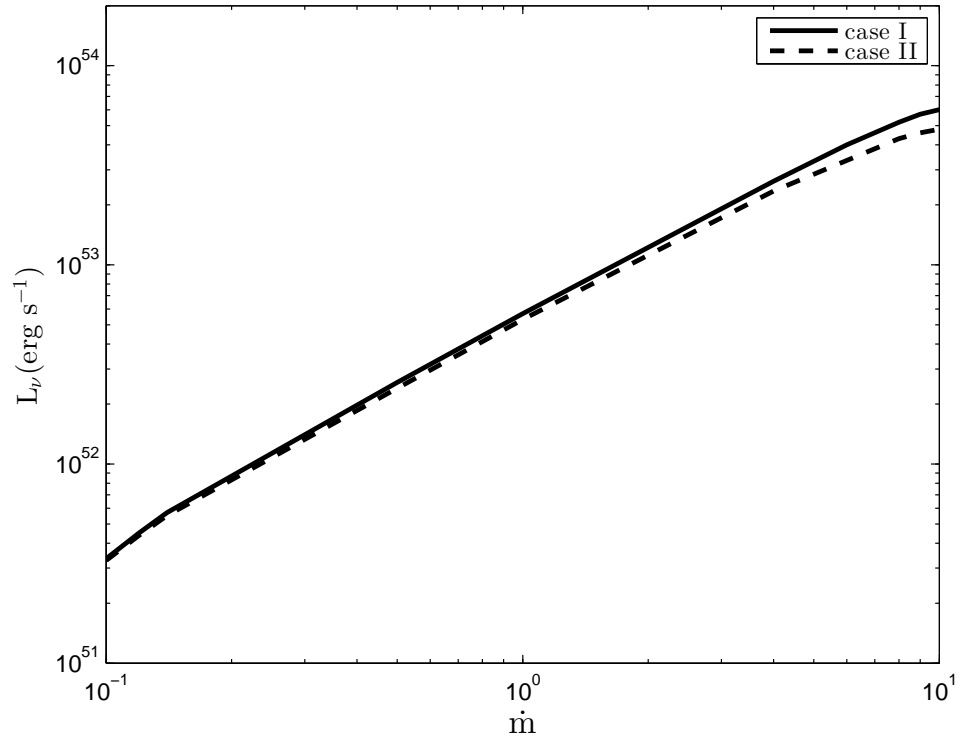


Fig. 6.— Neutrino luminosity L_ν for varying \dot{m} from 0.1 to 10.